Article

Neuron

Mitochondria Localize to Injured Axons to Support Regeneration

Highlights

- Axon injury increases mitochondria flux and axonal mitochondria density
- Robust mitochondria density is critical for axon regeneration
- Mitochondrial ATP production supports axon regeneration
- The DLK-1 MAP kinase pathway regulates axonal mitochondria density

Authors

Sung Min Han, Huma S. Baig, Marc Hammarlund

Correspondence

marc.hammarlund@yale.edu

In Brief

Han et al. find that axon injury and activation of DLK-1 MAP kinase increase axonal mitochondria density. Robust mitochondria density is required to produce adequate ATP for axon regeneration.

Han et al., 2016, Neuron *92*, 1308–1323
December 21, 2016
http://dx.doi.org/10.1016/j.neuron.2016.11.025

CellPress

CellPress

Neuron
Article

Mitochondria Localize to Injured Axons to Support Regeneration

Sung Min Han,[1] Huma S. Baig,[1] and Marc Hammarlund[1,2,*]
[1]Departments of Genetics and Neuroscience, Yale University School of Medicine, 333 Cedar Street, New Haven, CT 06510, USA
[2]Lead Contact
*Correspondence: marc.hammarlund@yale.edu
http://dx.doi.org/10.1016/j.neuron.2016.11.025

SUMMARY

Axon regeneration is essential to restore the nervous system after axon injury. However, the neuronal cell biology that underlies axon regeneration is incompletely understood. Here we use in vivo, single-neuron analysis to investigate the relationship between nerve injury, mitochondrial localization, and axon regeneration. Mitochondria translocate into injured axons so that average mitochondria density increases after injury. Moreover, single-neuron analysis reveals that axons that fail to increase mitochondria have poor regeneration. Experimental alterations to axonal mitochondrial distribution or mitochondrial respiratory chain function result in corresponding changes to regeneration outcomes. Axonal mitochondria are specifically required for growth-cone migration, identifying a key energy challenge for injured neurons. Finally, mitochondrial localization to the axon after injury is regulated in part by dual-leucine zipper kinase 1 (DLK-1), a conserved regulator of axon regeneration. These data identify regulation of axonal mitochondria as a new cell-biological mechanism that helps determine the regenerative response of injured neurons.

INTRODUCTION

Axon regeneration is a conserved mechanism in which neurons respond to axon injury by attempting to regrow and reconnect to their former postsynaptic targets. The success of axon regeneration is highly variable, even within neighboring neurons injured at the same time. It is also affected by multiple intrinsic and extrinsic factors that coordinately affect the motility, direction, morphology, and extension of the regenerating axons (Case and Tessier-Lavigne, 2005; Kerschensteiner et al., 2005). Within the injured neuron, axon regeneration involves multiple intracellular processes, including gene transcription, cytoskeletal rearrangements, and growth-cone formation (Bradke et al., 2012; Chisholm, 2013; Goldberg, 2003). Yet our understanding of the cell biology of axon regeneration is still incomplete. In particular, although many axon regeneration processes require energy, the functional relationship between mitochondria, nerve injury, and axon regeneration is not known.

Mitochondria are complex organelles with key functions in energy metabolism, calcium buffering, and signaling. Mitochondria change size and shape through regulated cycles of fission and fusion. In neurons, which have a highly extended morphology, mitochondrial position is regulated to satisfy local demands for energy or Ca^{2+} buffering, to respond to stressful conditions, and to remove damaged mitochondria (Cai et al., 2012; Chang and Reynolds, 2006; Hollenbeck and Saxton, 2005; Miller and Sheetz, 2004; Verburg and Hollenbeck, 2008; Wang et al., 2011). Mitochondrial subcellular localization and trafficking are mediated in neurons by microtubule-based motor proteins and accessory proteins, such as the mitochondrial protein Miro and the adaptor Milton (Hirokawa et al., 2010; Martin et al., 1999; Sheng, 2014; Wang et al., 2011). Functionally, the spatial and temporal regulation of mitochondria positioning in neurons is critical for neuronal development (Morris and Hollenbeck, 1993; Steketee et al., 2012), cortical axon branching (Courchet et al., 2013; Spillane et al., 2013), and presynaptic transmission (Sun et al., 2013). In vivo, mitochondria respond to axon injury by increased trafficking (Mar et al., 2014; Misgeld et al., 2007). In vitro, artificially increasing mitochondrial mobility increases axon growth in cultured cortical neurons (Zhou et al., 2016). Yet the contribution of mitochondrial traffic to regeneration in vivo is not clear, and the mechanisms that regulate the response of mitochondria to injury are incompletely understood.

In this study, we define the role of mitochondria during axon regeneration using the nematode *Caenorhabditis elegans* (*C. elegans*). We show that nerve injury results in translocation of mitochondria to the injured axon. Mitochondria density is a critical determinant of regeneration success, in particular for the growth phase of regeneration. Injured axons are in a state of energy stress, and proper mitochondrial respiratory chain function is critical for axon regeneration. Finally, we show that the conserved DLK-1 regeneration pathway promotes mitochondria localization to axons. An accompanying paper (Cartoni et al., 2016) shows that expression of the mitochondrial protein Armcx1 enhances both mitochondria transport and axon regeneration. Thus, mitochondria localization is a critical factor in axon regeneration.

RESULTS

Axon Injury Increases Mitochondria Density in Axons in Part by Increasing Transport

To analyze in vivo mitochondria behavior in individual axons after axon injury, we labeled mitochondria with mCherry

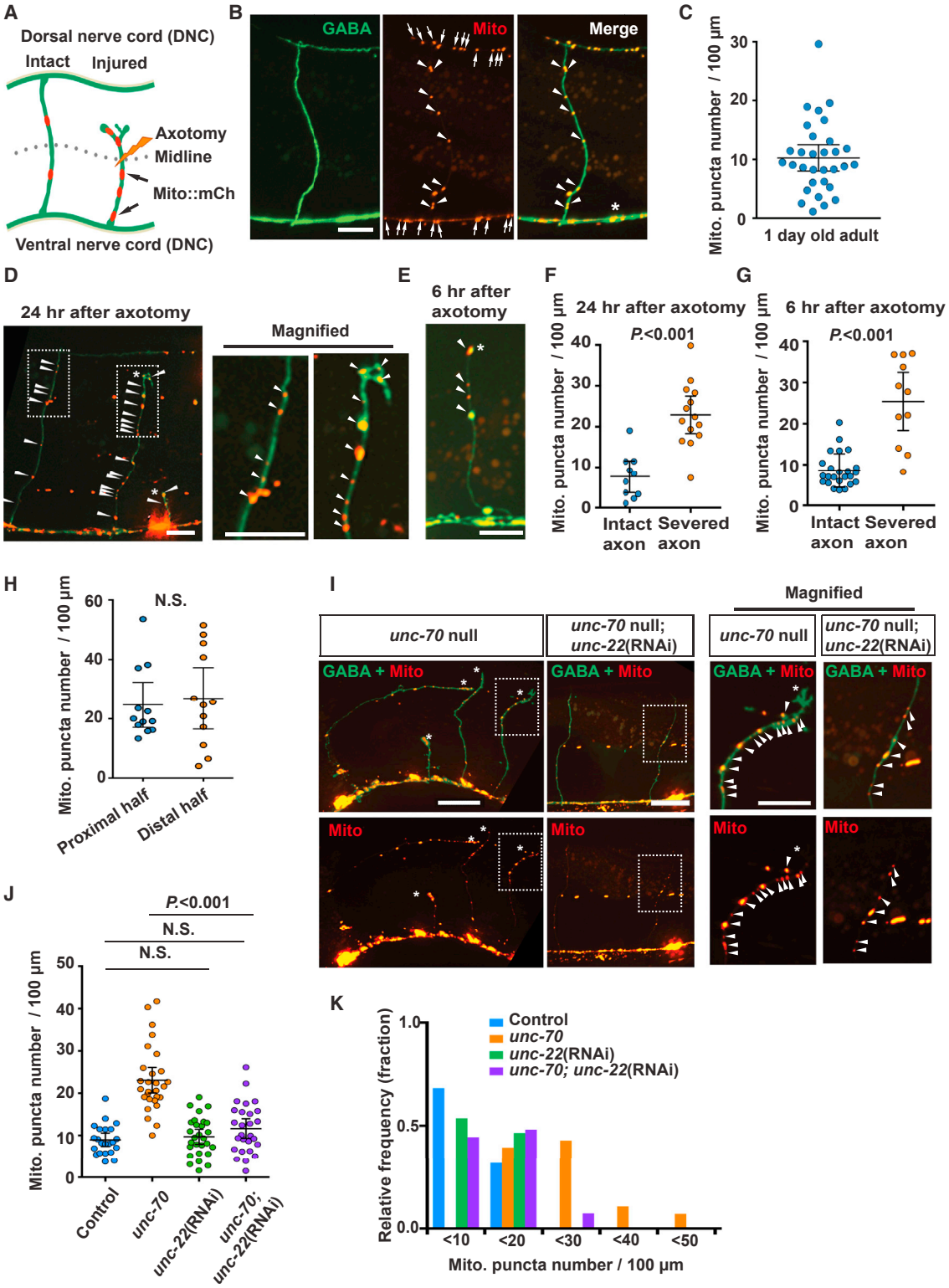

Figure 1. Axon Injury Increases Mitochondria Density in the Injured Axon

(A) Diagram of *C. elegans* GABA motor neurons showing mitochondria in intact and severed axons.

(B) Mitochondria in intact GABA axons of adult control animals. Arrowheads indicate individual mCherry puncta; mCherry is conjugated to the mitochondrial targeting sequence of TOM-20. Scale bar, 10 µm.

(legend continued on next page)

(Mito::mCherry) in the GABA motor neurons of *C. elegans*. These neurons are a well-established model for axon regeneration (Byrne et al., 2011; Hammarlund et al., 2009; Yanik et al., 2004), and coexpression of cytosolic GFP allowed both for analysis of overall neuronal morphology and for single-neuron laser axotomy (Figures 1A and 1B). In intact neurons, mitochondria were abundant in the cell body and were also enriched in puncta in the ventral (VNC) and dorsal (DNC) nerve cords likely corresponding to synaptic regions (Figure 1B). These data were consistent with previous results obtained both from fluorescent labeling and from electron microscopy reconstructions (Hall and Altun, 2008; Rawson et al., 2014). By contrast, axon commissures, which are asynaptic, contained few mitochondria. We defined mitochondria density in individual axons as the number of mitochondria puncta per 100 μm of axon, as assessed along the entire commissural axon from the ventral to the dorsal nerve cord. The average mitochondria density was 10.26 ± 2.23 per 100 μm axon length (mean ± 95% confidence intervals, n = 31) (Figures 1B and 1C). Mitochondria labeled with a different fluorophore and targeting sequence (mitochondria-matrix-targeted GFP) had a similar mitochondrial distribution, indicating that the observed mitochondria density and localization was independent of labeling effects (data not shown).

Next, we determined whether mitochondrial localization in the commissural axons is altered by injury (Figure 1A). We severed axons at the midline between the ventral and dorsal nerve cord with a pulsed laser and imaged the injured axons at 24 hr after injury (Byrne et al., 2011; Hammarlund et al., 2009; Yanik et al., 2004). Compared to intact axons, severed axons had about a 2-fold increase in mitochondria density (Figures 1D and 1F; Table S1). Increased mitochondria density in injured axons was also observed 6 hr after injury (Figures 1E and 1G; Table S1). Within the commissures of injured axons, the increase in mitochondria density within the proximal half of the commissural axon (closer to the ventral nerve cord and the cell body) was similar to the increase in the distal half of the commissural axon (closer to the axon stump and the eventual growth cone) (Figure 1H). The balanced increase in density makes simple spillover from the cell body unlikely and suggests that axon injury actively triggers mitochondrial localization to axons, rather than stabilization at a particular subcellular location.

To determine whether the increase in mitochondria density depends on the mode of injury, we measured mitochondria density in *unc-70/β-spectrin* mutants, which have spontaneous axon breakage due to mechanical stress from body bending (Hammarlund et al., 2000, 2007). Mitochondria density was higher in the damaged axons of *unc-70/β-spectrin* mutants. Further, the increased mitochondria density in *unc-70* mutants was suppressed by *unc-22/twitchin* RNAi, which prevents body bending and axon breakage (Figures 1I–1K; Table S1). Together, these data indicate that neurons respond to axon injury by increasing mitochondria density.

Increased mitochondria density could be a result of changes in mitochondrial translocation. Alternatively, increased density could be a result of increased mitochondria fission or decreased degradation of mitochondria mediated by mitophagy. To distinguish between these possibilities, we analyzed whether axon injury increases mitochondrial translocation into commissural axons from the ventral nerve cord, which contains the neuronal cell bodies and proximal axons. We established an in vivo system that allows selective labeling of VNC mitochondria using Mito::Dendra2 and that still allows visualizing axons for single-neuronal laser axotomy. Dendra2 is a photoconvertible fluorescent protein that irreversibly changes its fluorescent state from green to red in response to short wavelength light (405 nm). To test the specificity of our approach, we generated transgenic animals expressing Mito::Dendra2 in GABA neurons (Figure S1A). We selectively photoconverted the Mito-Dendra2 in the ventral nerve cord (VNC). After photoconversion, we found that red signal was found exclusively in the VNC (Figures S1A, S1C, and S1D; Table S1). Thus, our photoconversion approach allows us to specifically tag VNC mitochondria. Because gentle photoconversion was necessary to preserve neuronal health, only a portion of VNC mitochondria was marked with red. Next, in order to visualize axons for laser axotomy, we generated transgenic animals expressing both Mito::Dendra2 and cytosolic GFP in GABA neurons. As the cytosolic GFP (green) masks the green signal of unphotoconverted Mito::Dendra2, only photoconverted (red) Mito::Dendra2 can be observed. To test whether laser axotomy itself (performed at a wavelength of 440 nm) results in unwanted photoconversion, we cut axons and assessed red fluorescence immediately after injury. We found that axotomy resulted in little or no red signal, indicating that it did not significantly photoconvert Mito-Dendra2 (Figures S1B–S1D; Table S1). Thus, this system allows the tracking of mitochondria deriving from the VNC in the context of laser axotomy.

To determine whether axon injury results in increased translocation into commissural axons from the VNC, we converted VNC

(C) Scatterplot showing mitochondria density in individual intact GABA axons. Each dot indicates a single axon. Number of scored axons is 32.
(D and E) Mitochondria in GABA neurons at 24 hr after axotomy (D) and at 6 hr after axotomy (E). The right panels are magnified images of boxed areas. Asterisks indicate the tip of the regenerating axon. Arrowheads indicate individual mCherry puncta. Scale bars, 10 μm.
(F and G) Scatterplot showing mitochondria density in individual GABA axons at 24 hr after axotomy (F) and at 6 hr after axotomy (G). Dots indicate individual axons. Error bars indicate 95% confidence interval. Statistical significance was calculated by the Mann-Whitney test.
(H) Scatterplot showing mitochondria density in the proximal half (below DV, closer to the cell body) and the distal half (over DV, further from the cell body) of regenerating GABA axons 12 hr after injury. Dots indicate individual axons. Error bars indicate 95% confidence interval. Statistical significance was calculated by the Mann-Whitney test.
(I) Mitochondria in GABA neurons of *unc-70(s1502)* mutants. Images on right are magnified images of boxed areas. Asterisks indicate the tips of the regenerating axons. Arrowheads indicate individual mito-mCherry puncta. Scale bars, 20 μm.
(J) Scatterplot showing mitochondria density in GABA axons of indicated animals. Dots indicate individual axons. Error bars indicate 95% confidence interval. Statistical significance was calculated by the Mann-Whitney test.
(K) Binned frequency graph showing mitochondria density in the GABA axons of controls and *unc-70(s1502)* mutants. In each interval, a color-coded bar shows the fraction of axons with the given mitochondrial density.

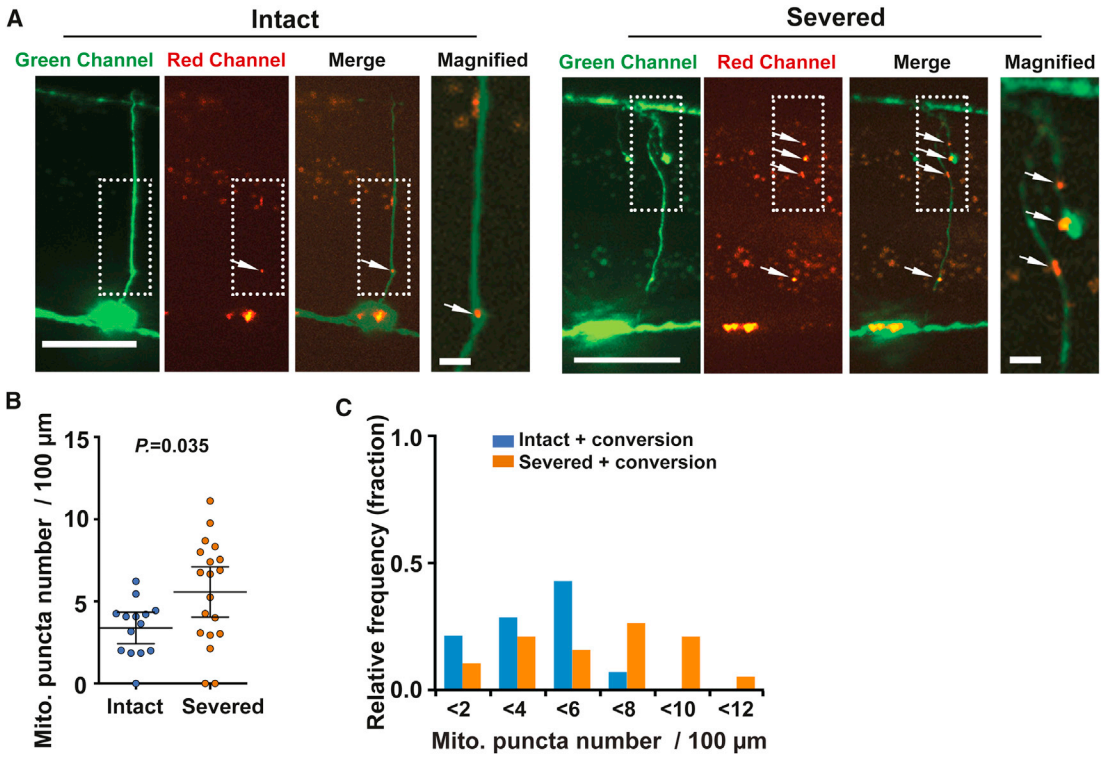

Figure 2. Axon Injury Increases Mitochondrial Translocation to the Axon Commissure

(A) Mitochondria in injured or intact GABA neurons at 24 hr after axotomy. Images on right are magnified images of boxed areas. Mitochondria are labeled with unconverted (green) mito::Dendra2. Green-mito::Dendra2 puncta on ventral nerve cords were specifically photoconverted (see Figure S2) to red color shortly after axotomy. Arrowheads indicate individual red-mito::Dendra2 puncta in the axons. Scale bars, 20 µm.

(B) Scatterplot showing red-mito::Dendra2 density in GABA axons 24 hr after axotomy and photoconversion. Dots indicate red-mito::Dendra2 puncta number in individual axons. Error bars indicate 95% confidence interval. Statistical significance was calculated by the Mann-Whitney test.

(C) Binned frequency graph of red-mito::Dendra2 density in GABA axons 24 hr after axotomy and photoconversion. For each segment, a color-coded bar shows the fraction of axons with given density of mitochondria that derive from the VNC.

mitochondria and imaged 24 hr later. At 24 hr, uninjured axons had significant numbers of red mitochondria in commissures compared to uninjured axons immediately after conversion, indicating that some VNC mitochondria translocate into the axon commissure in intact axons. By contrast, when axons were severed just after photoconversion, the mitochondria density 24 hr later was significantly higher than in uninjured axons (Figures 2A–2C; Table S1). These data indicate that axon injury results in increased mitochondria translocation from the VNC to the axon commissure.

As expected, due to the fact that gentle photoconversion results in incomplete mitochondria labeling, the density of commissural mitochondria observed with the photoconversion approach (both in uninjured and injured axons) (Figures 2B and 2C) was lower than the density observed with stable fluorophores under the same conditions (Figure 1F). However, this result also leaves open the possibility that a fraction of the mitochondria increase is due to other mechanisms besides translocation. We tested the idea that reduced mitophagy or increased mitochondrial division could contribute to increased mitochondria density in commissural axons after injury. To determine the effect of mitophagy, we examined axonal mitochondria density in a mitophagy-defective mutant. *pdr-1* is the *C. elegans* Parkin homolog and is required for mitophagy (Palikaras et al., 2015). We found that axonal mitochondria density in intact axons of *pdr-1* mutant animals was comparable to that of control animals (Figures S2A–S2C; Table S1), suggesting that blocking mitophagy is not sufficient to increase mitochondria density in axons. Furthermore, axon injury increased axonal mitochondria density in *pdr-1* mutant animals, indicating that mitophagy is not required to increase axonal mitochondria density after injury (Figures S2A–S2C; Table S1).

Next, to determine whether mitochondria division is increased by axon injury, we measured the size of mitochondria puncta. Mitochondria fission reduces the size of mitochondria (Detmer and Chan, 2007). Thus, if fission contributes to increased mitochondria density after axon injury, we would expect mitochondria size to be reduced. However, injury had no effect on mitochondria puncta size (Figures S2D–S2F), suggesting that fission is not increased in response to injury and does not significantly contribute to increased mitochondria density in response to injury. We conclude that relocalization of mitochondria from the VNC to the commissure is the primary cause of increased mitochondria density after injury.

AMP-activated protein kinase (AMPK) senses cellular energy status to maintain energy homeostasis and acts as a major

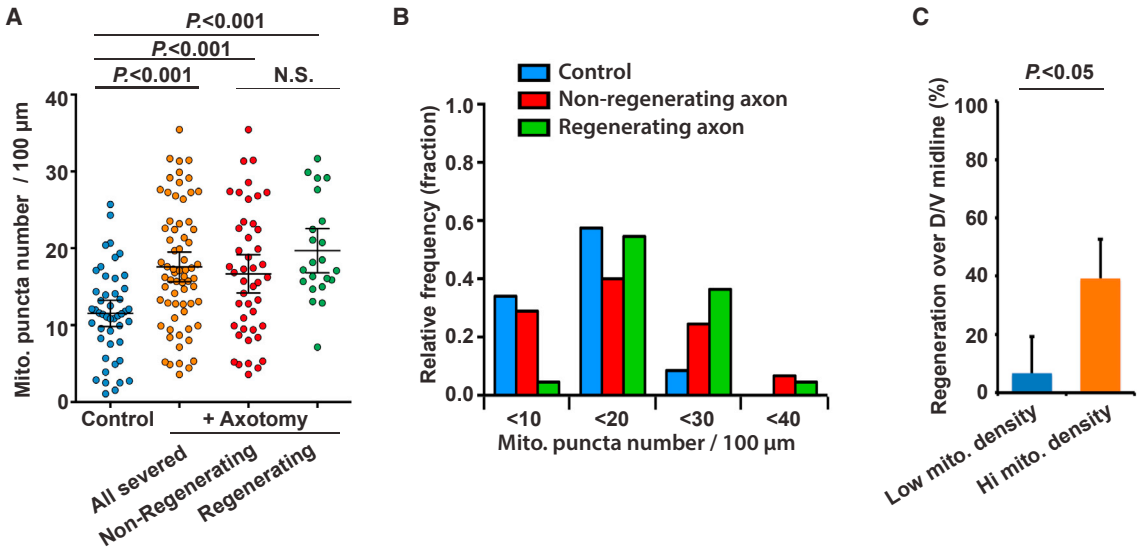

Figure 3. Mitochondria Density Correlates with Axon Regeneration

(A) Scatterplot showing mitochondria density in GABA axons 12 hr after axotomy. Dots indicate individual axons. Error bars indicate 95% confidence interval. Statistical significance was calculated by the Mann-Whitney test.

(B) Binned frequency graph of mitochondria density in GABA axons 12 hr after axotomy separated by regeneration outcome. For each segment, a color-coded bar shows the fraction of axons with given density of mitochondria.

(C) Regeneration of axons with mitochondria density >11 (hi mito. density) or with mitochondria density ≤11 (low mito. density) 24 hr after axotomy. Error bars indicate 95% confidence interval. Statistical significance was calculated by Fisher's exact test.

regulator of mitochondria (Hardie, 2007; Kahn et al., 2005). The *C. elegans* genome encodes two orthologs of the AMPK α catalytic subunits, AAK-1 and AAK-2. However, AAK-2 appears to be functionally more important, as *aak-2* mutations affect longevity, stress response, and reproduction, but mutation of *aak-1* does not cause obvious defects (Apfeld et al., 2004; Curtis et al., 2006; Lee et al., 2008). Consistent with previous findings, we found that mutation of *aak-2* caused reduced axon regeneration, whereas mutation of *aak-1* had no effect (Figures S3A and S3B) (Hubert et al., 2014; Nix et al., 2014). However, *aak-2* mutants exhibited indistinguishable mitochondria density in axons with or without injury compared to controls (Figures S3C and S3D; Table S1). Similar results were observed for *aak-1* mutants. These data indicate that the axon regeneration phenotype of *aak-2* mutants is not due to changes in mitochondria density or translocation.

Mitochondria Density in Individual Axons Is Associated with Axon Regeneration

The increase in mitochondria density in axons after injury suggests that increased mitochondrial localization to the injured axon may support axon regeneration. Like mitochondrial localization (Figure 1), axon regeneration after injury is a highly variable process at the level of individual neurons. Under standard experimental conditions, approximately 70% of injured GABA axons manifest a successful growth cone and 30% fail (Hammarlund et al., 2009; Yanik et al., 2004). We examined mitochondria density in individual severed axons 12 hr after injury and also assessed axon regeneration of the same individual neurons (Figure 3A). While on average injured axons had increased mitochondria density compared to intact axons, in individual axons there was substantial overlap in mitochondria density between intact and injured axons. However, when only injured axons were considered and partitioned into those that had regenerated and those that had not, we observed a striking difference in mitochondria density between individual regenerating and nonregenerating axons. In regenerating axons, the distribution of mitochondria densities was skewed away from the lower end. Only 1 out of 21 individual regenerating axons had a mitochondria density less than the median density in intact control axons (11 puncta per 100 μm), whereas 14 of 45 nonregenerating axons had a mitochondria density of less than 11 per 100 μm (Figures 3A and 3B). Thus, axons with low mitochondria density are unlikely to regenerate (6.6%, or 1 of 15 axons with density lower than 11 per 100 μm) compared to axons with high mitochondria density (39.2%, or 20 of 51 axons with density higher than 11 per 100 μm) (Figure 3C). Thus, increased mitochondria density is necessary for robust regeneration. Despite these differences, in both regenerating and nonregenerating axons, average mitochondria density increased compared to uninjured axons, and a substantial number of individual axons in both categories achieved high mitochondria density (Figure 3A). These data indicate that increased mitochondria density is necessary, but not sufficient, for successful regeneration: even axons with high individual mitochondria density may fail to regenerate, but axons with low mitochondria density are very unlikely to do so.

Axonal Mitochondria Are Required for Proper Axon Regeneration

To confirm the idea that low mitochondria density results in poor regeneration, we tested whether inhibition of mitochondrial

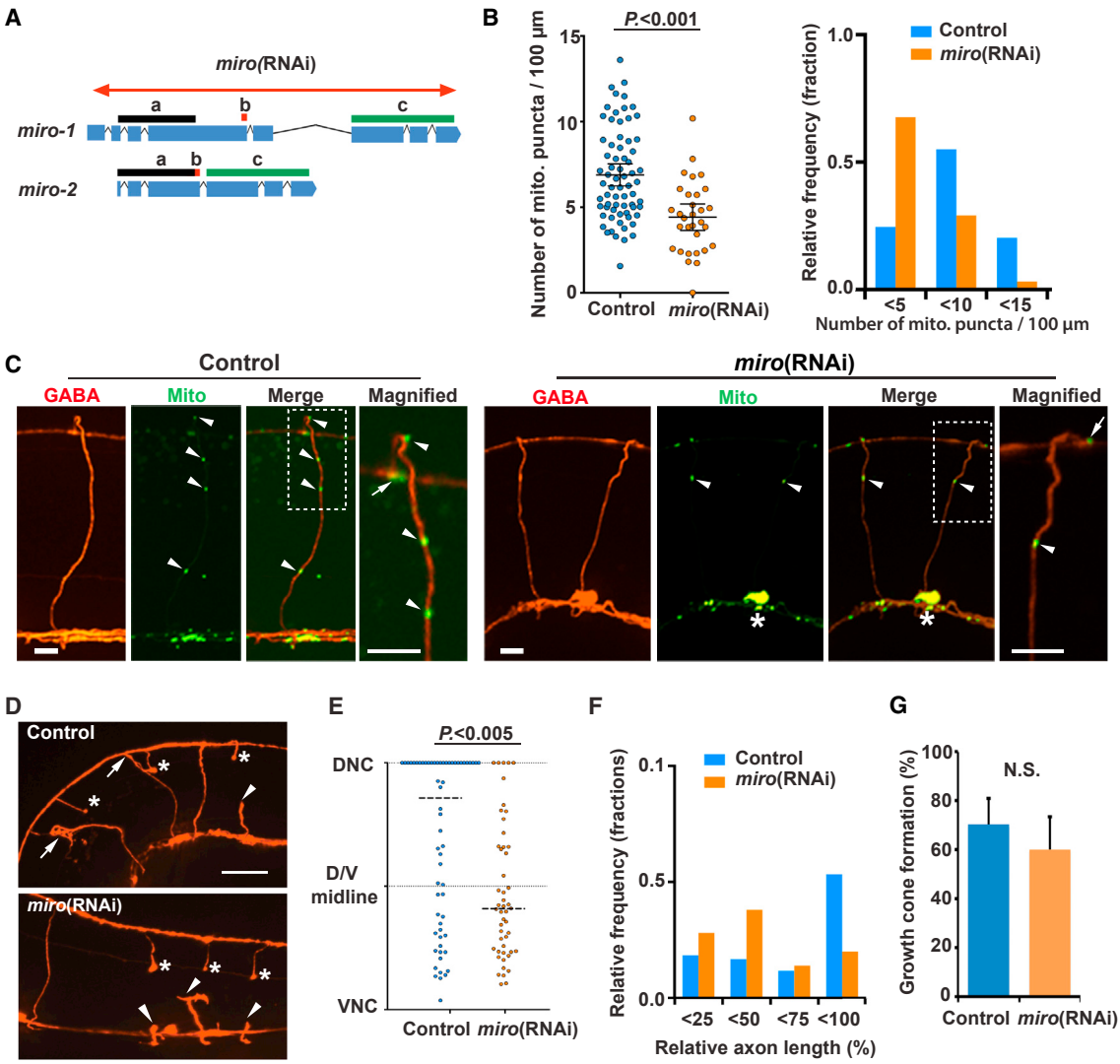

Figure 4. Decreasing Axonal Mitochondria Reduces Axon Regeneration

(A) Diagram showing genetic loci for *miro-1* and *miro-2* and the *miro* RNAi targeting area. Bars (a, b, and c) indicate areas with 100% identical nucleotide sequence.

(B) Scatterplot (left) and binned frequency graph (right) showing mitochondria density in GABA axons of L4-stage animals with or without GABA-specific *miro* RNAi. Bars indicate average ± 95% confidence interval. Statistical significance was calculated by the Mann-Whitney test.

(C) Mitochondria in GABA neurons of control and *miro(RNAi)* animals. Images on right are magnified images of boxed areas. Asterisks indicate cell body. Arrowheads indicate individual mito::GFP puncta within individual axon commissure. Arrows indicate mito::GFP puncta in dorsal nerve cord. Scale bars, 5 µm.

(D) GABA axons 24 hr after axotomy in control and *miro(RNAi)* animals. Arrows indicate successful regeneration, arrowheads indicate failed regeneration, and asterisks indicate distal stumps that confirm axotomy. Scale bar, 20 µm.

(E and F) Scatterplot (E) and binned frequency graph (F) of relative axon length of GABA axons 24 hr after axotomy. Dots indicate individual axons, and lines indicate median. n = 71 (control) and 50 (*miro* RNAi). Horizontal dashed lines indicate median. Statistical significance was calculated by the Mann-Whitney test.

(G) Growth-cone formation 24 hr after axotomy. Error bars indicate 95% confidence interval. Statistical significance was calculated by Fisher's exact test.

transport in axons affects axon regeneration after injury. Miro is a mitochondrial outer membrane GTPase that is specifically required for mitochondrial transport (Fransson et al., 2003; Guo et al., 2005). The *C. elegans* genome encodes two Miro homologs, *miro-1/K08F11.5* and *miro-2/C47C12.4*. In MIRO-1, 97% of the MIRO-2 amino acid sequence is conserved, suggesting that these genes may have a redundant function in mitochondrial transport (Figure 4A). To inhibit both *miro-1* and *miro-2* function exclusively in GABA neurons, we performed GABA-specific RNAi (Firnhaber and Hammarlund, 2013) against both *miro-1* and *miro-2* (Figure 4A). *miro* RNAi animals showed reduced mitochondria density in GABA commissures (Figures 4B and 4C; Table S1). Thus, *C. elegans* Miro has a conserved function in mitochondrial axon transport. Next, we assessed axon

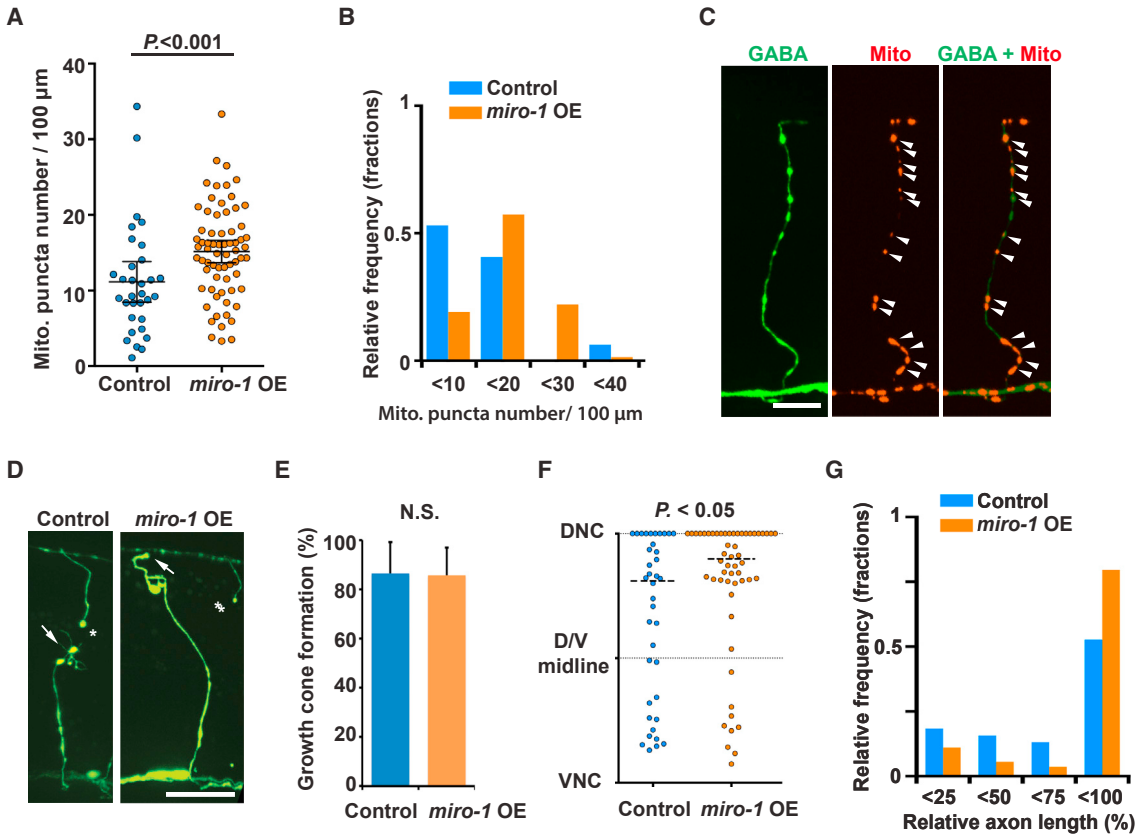

Figure 5. Increasing Axonal Mitochondria Improves Axon Regeneration

(A and B) Scatterplot (A) and binned frequency graph (B) showing mitochondria density in GABA axons of L4-stage control and *miro-1* OE animals. Bars indicate average ± 95% confidence interval. Statistical significance was calculated by the Mann-Whitney test.

(C) Mitochondria in GABA neurons of animals with *miro-1* overexpression in GABAergic neurons. Arrowheads indicate individual mito::mCherry puncta. Scale bar, 20 µm.

(D) GABAergic axons 24 hr after axotomy in control and *miro-1* OE animals. Arrows indicate successful regeneration; asterisks indicate distal stumps that confirm axotomy. Scale bar, 20 µm.

(E) Growth-cone formation 24 hr after axotomy. Error bars indicate 95% confidence interval. Statistical significance was calculated by Fisher's exact test.

(F and G) Scatterplot (F) and binned frequency graph (G) of relative axon length of GABA axons 24 hr after axotomy. Dots indicate individual axons, and lines indicate median. n = 38 (control) and 55 (*miro-1* OE). Horizontal dashed lines indicate median. Statistical significance was calculated by the Mann-Whitney test.

regeneration in *miro* RNAi animals and found that reduction of Miro resulted in reduced regeneration across the dorsal-ventral body midline and reduced regrowth to the dorsal nerve cord (Figures 4D and 4E). The overall length of regenerated axons was shorter in *miro* RNAi animals (Figures 4D–4F). Therefore, mitochondrial transport is critical for axon regeneration. Detailed analysis of regeneration showed that, although *miro* RNAi results in defective axon extension, *miro* RNAi and control animals have similar growth-cone formation (Figure 4G). Thus, axonal mitochondria are dispensable for injury signaling and growth-cone initiation but are required for robust regenerative growth.

As axonal mitochondria promote regeneration, we considered whether increasing axonal mitochondria density above normal levels might improve regeneration. Overexpression of Miro has been shown to influence motility or subcellular distribution of mitochondria in neuronal cultures and *Drosophila* neurons (Ahmad et al., 2014; Guo et al., 2005; Saotome et al., 2008). Further, overexpressing Miro results in increased mitochondrial motility and increased growth in cultured cortical neurons (Zhou et al., 2016). Consistent with these results, we found that overexpression of *miro-1* in GABA neurons resulted in increased mitochondria density (Figures 5A–5C; Table S1). Next, we tested the effect of *miro-1* overexpression on axon regeneration. After injury, *miro-1* overexpression did not affect growth-cone formation (Figure 5E) but resulted in longer axon lengths compared to controls (Figures 5D, 5F, and 5G). Thus, manipulation of the mitochondria transport factor Miro results in changes in axonal mitochondria density and in corresponding changes in axon regeneration.

As an alternative approach to Miro manipulation to test the importance of axonal mitochondria for axon regeneration, we examined animals with abnormal mitochondrial fission. Dynamin-related protein 1 (DRP-1) is a member of the dynamin family of large GTPases that regulate mitochondrial fission (Labrousse et al., 1999). In *Drosophila* neurons, loss of DRP-1 function results in hyperfused mitochondria that fail to traffic to synapses

(Verstreken et al., 2005). However, mitochondrial membrane potential and cellular ATP level remain largely unaffected in multiple studies (Lathrop and Steketee, 2013; Verstreken et al., 2005; Wakabayashi et al., 2009). We found that in the GABA neurons of *drp-1* mutants, mitochondria were mainly confined to the cell body. Mitochondria were largely depleted from axons and synapses. Elongated mitochondria were visible in some axons, consistent with hyperfusion (Figure S4A). The abnormal distribution and the shape of mitochondria distribution in *drp-1* mutants were rescued by GABA-specific expression of wild-type *drp-1* (Figure S4A). Despite their mitochondrial defects, *drp-1* null mutants exhibit normal GABA neuron morphology. We found that, after single-neuron laser axotomy, *drp-1* mutants had defects in axon regeneration similar to *miro* RNAi. While growth-cone formation in *drp-1* mutants was similar to that found in control animals (Figure S4C), *drp-1* mutants had reduced axon regeneration over the dorsal-ventral body midline and to the dorsal nerve cord (Figures S4B and S4D). The overall length of regenerated axons was also shorter in *drp-1* mutants (Figures S4E and S4F). Consistent with *drp-1*'s effect on mitochondrial localization (Figure S4A), GABA-specific expression of wild-type *drp-1* rescued the axon regeneration defects in *drp-1* null mutants (Figures S4D and S4G). Taken together, our data on *Miro* and *drp-1* demonstrate that manipulation of mitochondria density causes corresponding changes in long-distance axon regeneration, consistent with the idea that axon regeneration is critically dependent on increased mitochondria density.

Proper Mitochondrial Respiratory Chain Function Is Required for Normal Axon Regeneration

Mitochondria are multifunctional organelles that mediate energy metabolism, calcium homeostasis, regulation of reactive oxygen species (ROS) level, and other functions (Lin and Sheng, 2015). We hypothesized that mitochondrial function in energy metabolism is specifically important for injured axon regrowth, and that axons that lack sufficient mitochondria have reduced axon regeneration due to energy deficits. To test the hypothesis that axon regeneration depends on energy production by mitochondria, we assessed axon regeneration in animals with defective mitochondrial respiratory chain function. *nuo-6* (a subunit of complex I) and *isp-1* (a subunit of complex III) encode subunits of mitochondrial respiratory complexes. Partial loss-of-function mutations in these genes result in reduced energy production, as assessed by decreased ATP levels and oxygen consumption. Of the two mutants, *isp-1(qm150)* has lower ATP levels than *nuo-6(qm200)*, making this a useful system for testing the relationship between energy levels and axon regeneration (Yang and Hekimi, 2010; Yee et al., 2014). We analyzed axon regeneration in these mutant animals 24 hr after axotomy. Like the regeneration defects caused by alterations in mitochondria density (Figures 3–5), the *isp-1(qm150)* and *nuo-6(qm200)* mutations resulted in reduced regrowth over the midline and less full regeneration to the dorsal nerve cord (Figures 6A and 6B). Further, *isp-1* mutants had a lower axon regeneration rate than *nuo-6* mutants, consistent with the different ATP levels between *isp-1* mutants and *nuo-6* mutants (Figures 6A and 6B; Yang and Hekimi, 2010; Yee et al., 2014). Neither *isp-1* nor *nuo-6* mutants had abnormal mitochondrial positioning in the axon (Figures S5A–S5C; Table S1). As in control animals, axon injury increases mitochondrial density in *nuo-6* mutants (Figures S5D–S5F). These observations indicate that positioning of mitochondria with proper energy production in axons is required for efficient axon regeneration after injury, and they support the idea that the major role of axonal mitochondria during regeneration is to supply adequate levels of ATP.

isp-1 and *nuo-6* mutants have mild increases in mitochondrial superoxide levels but have decreased oxidative damage to proteins, increased expression of the superoxide dismutases (Yang and Hekimi, 2010; Yang et al., 2007), and increased resistance to paraquat treatment (Yang and Hekimi, 2010). These results suggest that neither oxidative damage nor the cellular response to ROS is the cause of reduced regeneration in these animals (Hwang and Lee, 2011; Lee et al., 2010; Yee et al., 2014). We further tested whether a mild increase in ROS levels could affect axon regeneration (Figure S6A). Treatment with 0.5 mM paraquat has been shown to be sufficient to increase the expression of superoxide dismutases and mitochondrial chaperones and to cause a lifespan extension that recapitulates the lifespan extension of *nuo-6* and *isp-1* mutants (Lee et al., 2010; Runkel et al., 2013), suggesting that this treatment results in appreciable levels of ROS. Expression of *g*lutathione S-transferase 4 (*gst-4*) is upregulated in response to oxidative stress. We confirmed that treatment with 0.5 mM paraquat induced expression of a *gst-4* GFP reporter (Figure S6B; Tawe et al., 1998). However, paraquat treatment did not alter axon regeneration (Figure S6C). Consistent with our finding that ROS do not inhibit axon regeneration in *C. elegans*, it has been shown that in zebrafish, hydrogen peroxide promotes axon regeneration of peripheral sensory neurons (Hwang and Lee, 2011; Lee et al., 2010; Rieger and Sagasti, 2011; Yee et al., 2014).

Mitochondria also play critical roles in cytoplasmic Ca^{2+} buffering and Ca^{2+} homeostasis. Under normal conditions, the mitochondrial calcium uniporter (MCU) complex regulates Ca^{2+} entry into the mitochondrial matrix (Baughman et al., 2011; De Stefani et al., 2011). *mcu-1* is the sole MCU homolog in *C. elegans*, and loss of *mcu-1* strongly reduces mitochondrial Ca^{2+} uptake induced by epidermal wounding (Xu and Chisholm, 2014). We found that *mcu-1* mutants had normal levels of axon regeneration, indicating that impaired mitochondrial Ca^{2+} buffering after axotomy does not lead to axon regeneration defects (Figures S7A–S7D).

Together, these results support the model that energy production is the primary function of axonal mitochondria during axon regeneration. If this model is true, we hypothesized that regenerating axons might be in a state of energy crisis, consistent with our findings that alterations in mitochondria distribution and energy production have major effects on regeneration. We assessed energy status in axons using a GFP reporter of phosphofructokinase localization (PFK-1.1::eGFP). Phosphofructokinase is a key glycolytic enzyme, and PFK-1.1::eGFP forms clusters in neurons under diverse conditions that cause energy stress (Jang et al., 2016). Consistent with previous results, we found that PFK-1.1::eGFP clusters were rarely observed in intact GABA neurons under normal conditions. By contrast, after axon injury we found high levels of PFK-1.1::eGFP clusters, indicating that injured axons are under energy stress (Figures 6C–6E). However,

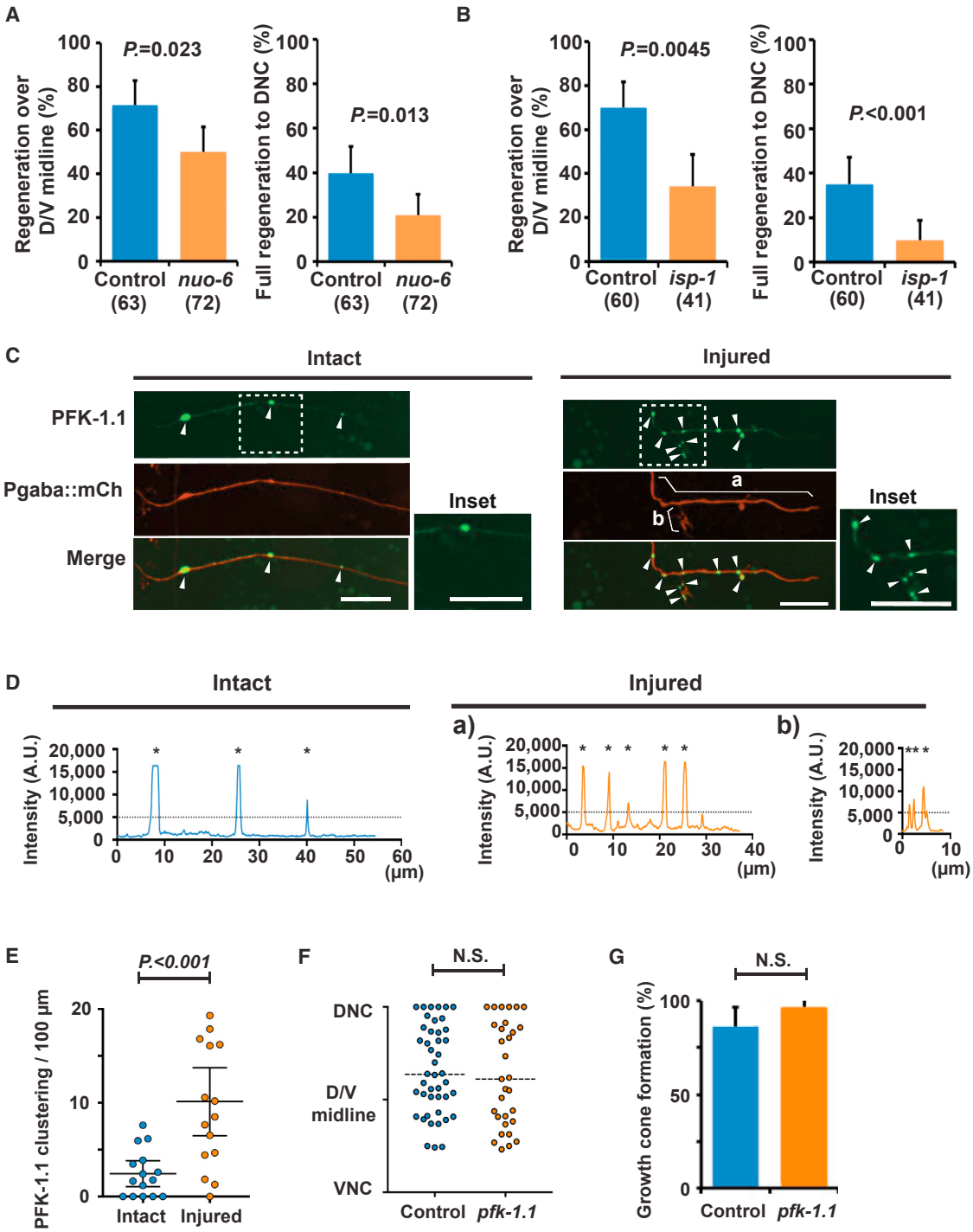

Figure 6. Axon Regeneration Requires Proper Mitochondrial Energy Production

(A and B) Regeneration over dorsal-ventral midline (left) and full regeneration to the dorsal nerve cord (right) of controls and both *nuo-6(qm200)* and *isp-1(qm150)* mutant animals 24 hr after axotomy. Error bars indicate 95% confidence interval. Statistical significance was calculated by Fisher's exact test. The numbers indicate the number of animals tested.

(C and D) Localization of PFK-1.1::GFP in GABA axon labeled with mCherry and its respective fluorescence intensity along the intact axons or the injured axons 24 hr after axotomy. (C) Arrowheads indicate PFK-1.1::GFP clusters. The insets are magnified images of boxed areas. For the injured axon, regions "a" and "b" are separately analyzed in (D). Scale bars, 10 μm. In (D), asterisks indicate the peaks with higher value than the threshold value. The dashed lines indicate threshold.

(E) Quantification of the PFK-1.1::GFP clusters in the axons with or without injury.

(legend continued on next page)

disrupting glycolysis by mutating *pfk-1.1* did not affect either long-distance axon regeneration or growth-cone formation after injury (Figures 6F and 6G). Thus, injured axons are in a state of energy crisis, and mitochondria—rather than glycolysis—are required to supply sufficient energy for regeneration.

DLK-1 Regulates Mitochondria Translocation after Injury

How does axon injury increase mitochondria density in injured axons? We hypothesized that increases in mitochondria density may be mediated by the DLK injury-signaling pathway. DLK-1 is a dual leucine zipper-bearing MAP kinase kinase kinase (MAPKKK) that is a key determinant of axon regeneration in *C. elegans,* mice and flies (Hammarlund et al., 2009; Nakata et al., 2005; Shin et al., 2012; Xiong et al., 2010; Yan et al., 2009; Figure 8A). In *C. elegans* GABA neurons, loss of *dlk-1* blocks axon regeneration, while DLK-1 overexpression enhances axon regeneration (Hammarlund et al., 2009; Yan et al., 2009). We tested whether *dlk-1* regulates mitochondria translocation. In intact axons, *dlk-1* mutants had mitochondria density that was indistinguishable from controls. By contrast, at 24 hr after axotomy, injured axons in *dlk-1* mutants had significantly lower mitochondria density than injured axons in controls (Figures 7A–7C; Table S1). While mitochondria density did increase in response to injury in *dlk-1* mutants, the average increase was smaller: control axons showed about a 1.9-fold increase in mitochondrial density after injury, and *dlk-1* mutant axons showed about a 1.5-fold increase. Further, in *dlk-1* mutants, 27.4% of individual injured axons had a mitochondria density below 10, compared to 6.9% in controls (Figure 7C). Axons with such a low mitochondria density are highly unlikely to regenerate (Figure 3C). Thus, DLK signaling is required for axons to translocate sufficient mitochondria into axons for regeneration competence, and multiple injury-signaling mechanisms, including DLK-1 signaling, regulate mitochondria density in injured axons.

DLK-1 Activation Is Sufficient to Increase Mitochondria Density in Axons

To confirm the finding that DLK-1 signaling increases mitochondria density in response to injury (Figures 7A–7C), we tested whether DLK-1 activity is sufficient to increase mitochondria density even in the absence of axon injury. Overexpression of the active form of DLK-1 results in constitutive activation and enhanced regeneration (Hammarlund et al., 2009; Yan and Jin, 2012). We found that overexpression of the active form of DLK-1 (DLK-1 OE) increased mitochondria density in uninjured axons (Figures 7D–7F; Table S1). By contrast, DLK-1 overexpression did not affect the axonal distribution or appearance of other organelles such as lysosomes, Golgi outposts, and synaptic vesicle precursors (Figures S8A–S8C). Thus, DLK-1 activity appears to specifically affect mitochondrial positioning in axons rather than global axonal transport. A major mediator of DLK-1 signaling is the bZip domain-containing protein CEBP-1 (Yan et al., 2009). We found that loss of *cebp-1* suppressed the increase in mitochondria density in animals overexpressing DLK-1 (Figures 7D–7F; Table S1). We conclude that activation of the canonical DLK-1 pathway is sufficient to increase mitochondria density in axons.

Both DLK overexpression and Miro overexpression result in increased mitochondria density and improved axon regeneration (Figures 5 and 7). DLK overexpression functions via *cebp-1* (Figure 7) (Yan et al., 2009), but downstream mechanisms are largely unknown. We tested the idea that DLK overexpression affects mitochondria and regeneration by increasing Miro-based mitochondria transport. We examined *miro-1; miro-2* double mutant animals either with or without *dlk-1* overexpression. Consistent with *miro(RNAi)* animals (Figure 4), *miro-1; miro-2* double mutants exhibited lower mitochondrial density than did wild-type animals (Figures 8A–8C). Further, *dlk-1* overexpression in *miro-1; miro-2* double mutants increased mitochondrial density in intact axons (Figures 8A–8C). Thus, Miro itself and Miro-dependent mechanisms of mitochondria transport are not required for the effect of DLK overexpression on axonal mitochondria density in intact neurons. Next, we severed axons and assessed regeneration. Consistent with previous studies, *dlk-1* overexpression in GABA neurons increased overall axon length, and a larger fraction of axons extended to near the dorsal nerve cord (between 75% and 100% of relative axon length) (Hammarlund et al., 2009). *miro-1; miro-2* double mutants, like *miro* RNAi (Figure 4), had reduced regeneration. However, *dlk-1* overexpression in *miro-1; miro-2* double mutants resulted in increased regeneration, similar to that found in *dlk-1*-overexpressing animals alone (Figures 8D–8F). Together, these results indicate that DLK-1 overexpression and Miro regulate both axon regeneration and mitochondria localization via two independent mechanisms.

DISCUSSION

We have investigated the relationship between axon injury, axonal mitochondria, and regeneration. We find that axon injury results in increased mitochondria density in injured axons. High mitochondria density in individual axons is required for regeneration, and experimentally altering mitochondria density results in corresponding effects on regeneration. Injured axons are in energy crisis, and of all mitochondria functions, only respiratory chain function is critical for axon regeneration, indicating that increased axonal mitochondria provide energy required for regeneration. Finally, the DLK-1 injury-signaling pathway specifically promotes increased mitochondria density, potentially by mechanisms independent of the Miro-based mitochondria trafficking complex. Together, these data establish functional links between nerve injury, mitochondria localization, and axon regeneration.

(F) Scatterplot of relative axon length of GABA axons 24 hr after axotomy in control and *pfk-1.1(gk922689)* mutants. Dots indicate individual axons. Horizontal dashed lines indicate median. Statistical significance was calculated by the Mann-Whitney test.
(G) Growth-cone formation 24 hr after axotomy. Error bars indicate 95% confidence interval. Statistical significance was calculated by Fisher's exact test. n = 46 (control) and 31 (*pfk-1.1(gk922689)*).

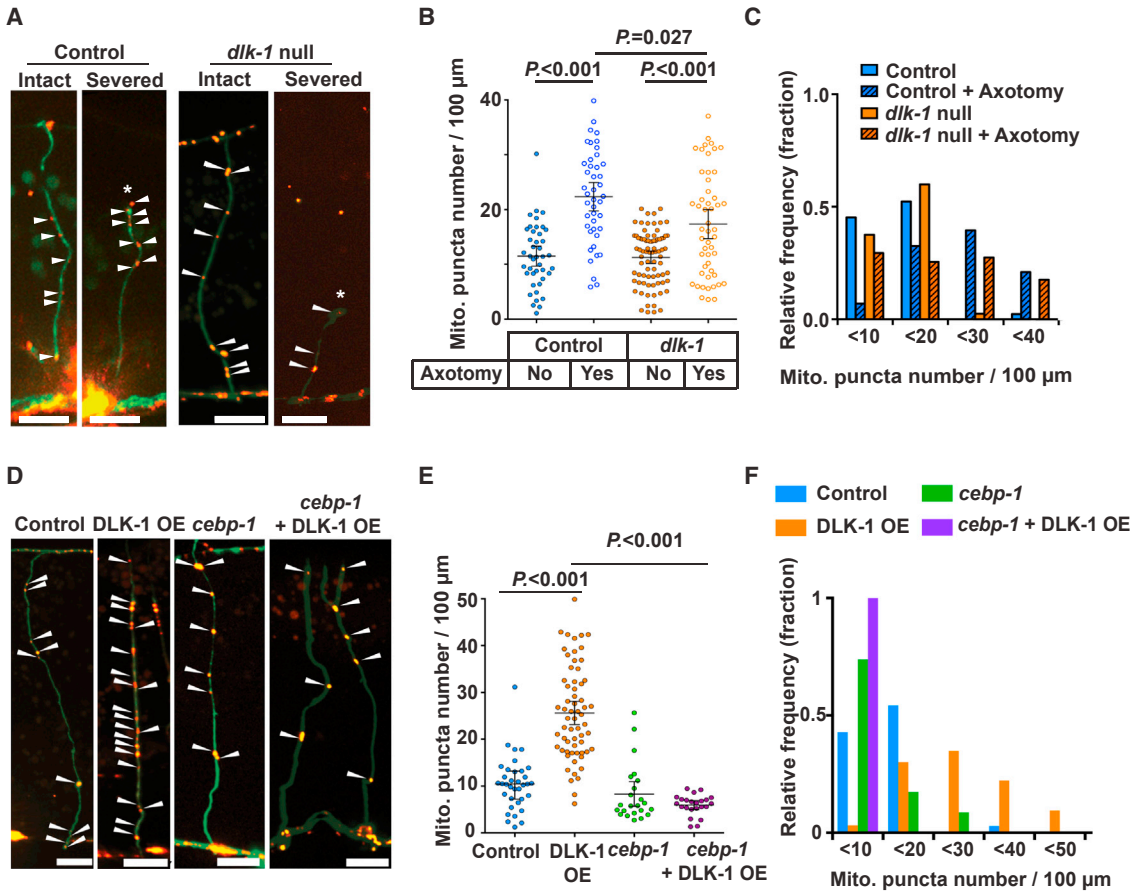

Figure 7. DLK-1 Regulates Mitochondria Density in Axons

(A) Representative micrographs of mitochondria in the GABA axons of *dlk-1(ju476)* mutants at 24 hr after axotomy. Arrowheads indicate single Mito::mCherry puncta. Scale bars, 10 µm.

(B) Scatterplot showing mitochondria density in GABA axons 24 hr after axotomy. Dots indicate individual axons. Error bars indicate 95% confidence interval. Statistical significance was calculated by the Mann-Whitney test.

(C) Binned frequency graph showing mitochondria density in GABA axons 24 after axotomy. After axotomy, compared to control (6.9%), *dlk-1* null mutants (29.4%) show a higher fraction of axons with mitochondrial density < 10 in the injured axons.

(D) Mitochondria in uninjured GABA axons. Arrowheads indicate single Mito::mCherry signals. Scale bars, 10 µm.

(E) Scatterplot showing increased mitochondria density in GABA axons due to DLK-1 overexpression. Dots indicate individual axons. Lines indicate means and error bars indicate 95% confidence interval. Statistical significance was calculated by the Mann-Whitney test.

(F) Binned frequency graph showing mitochondria density in intact GABA axons of given animals.

Axon Injury Triggers Increased Mitochondria Translocation to Axons

We find that *C. elegans* axon injury triggers a robust increase in mitochondria density in injured axons in vivo. Mitochondria density increases quickly after injury and is maintained to a late time point, when axon regeneration is complete. The distribution of mitochondria is uniform throughout the entire injured axon, including the growth-cone area. Two different modes of injury—laser axotomy and mechanical breakage—trigger increases in mitochondria density, indicating that mitochondria density is responding to injury itself, rather than to side effects of the injury method. Further, we found that injury results in increased mitochondria translocation from neuronal cell bodies and proximal axons to the more distal commissures, indicating that overall mitochondria flux during this period is anterogradely directed. Our data are consistent with studies in mice that demonstrated increased axonal mitochondria traffic after peripheral nerve injury (Mar et al., 2014; Misgeld et al., 2007), suggesting that a general response to axon injury across species is to increase translocation of mitochondria into injured axons through regulation of mitochondrial transport and flux. An open question is whether mitochondria translocation into axons is accompanied by mitochondrial biogenesis. One regulator of mitochondrial biogenesis is AMPK; we found that mitochondria density or translocation was unaffected by mutation of either of the *C. elegans* AMPK homologs, but further experiments are necessary to determine whether axon injury triggers a mitochondrial biogenesis response.

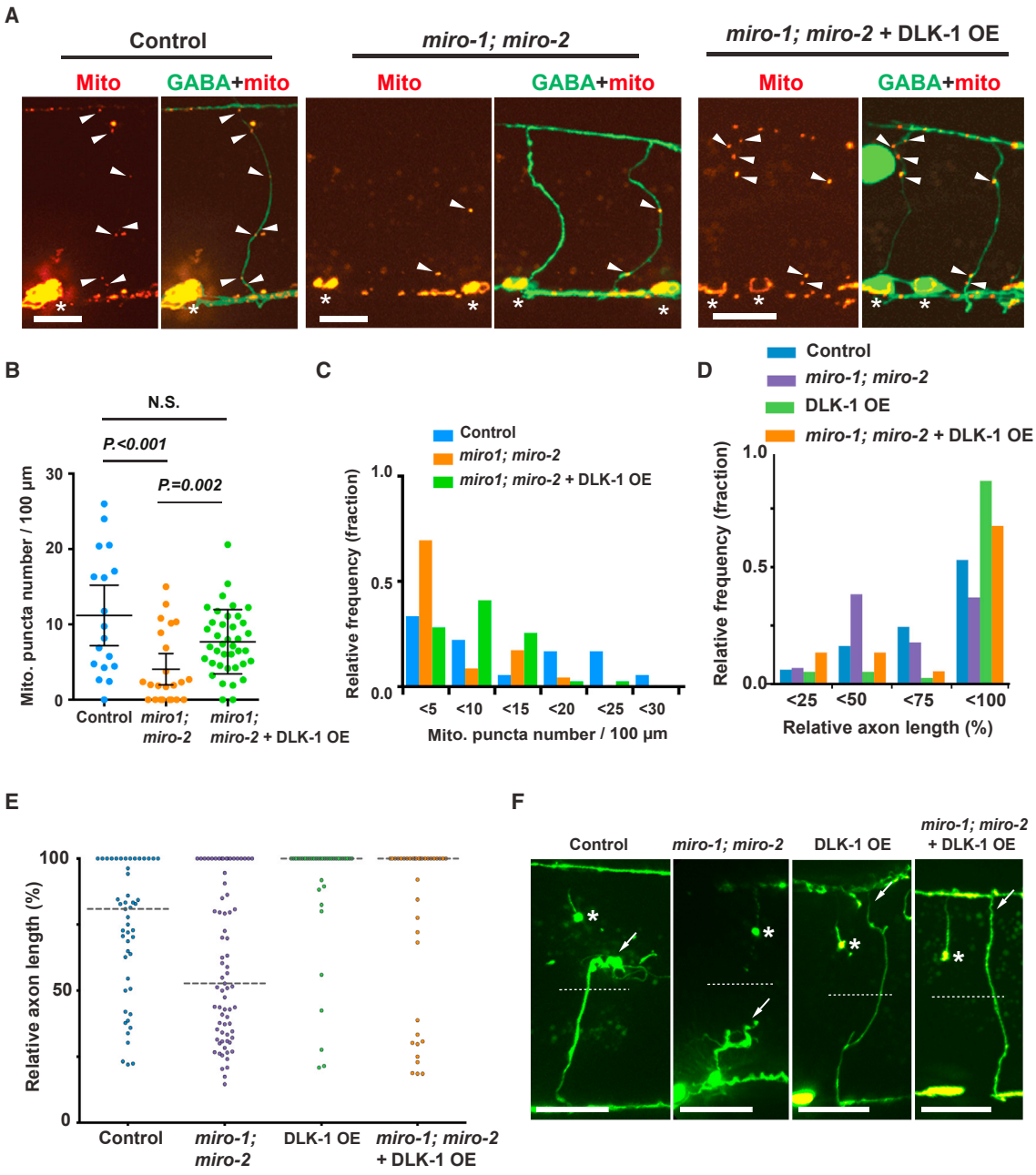

Figure 8. DLK-1 Overexpression Functions Independently of Miro

(A) Mitochondria in GABA neurons of given animals. Arrowheads indicate individual Mito::mCherry puncta. Scale bars, 10 µm.

(B and C) Scatterplot (B) and binned frequency graph (C) of mitochondria density of GABA axons 24 hr after axotomy. Dots in (B) indicate individual axons, and error bars indicate average ± 95% confidence interval. Statistical significance was calculated by the Mann-Whitney test.

(D and E) Binned frequency graph (D) and scatterplot (E) showing relative axon length of given animals 24 hr after axotomy. Dashed lines in (E) indicate median.

(F) GABAergic axons 24 hr after axotomy in given animals. Arrows indicate axon tips. Asterisks indicate distal stumps that confirm axotomy. Scale bars, 20 µm.

Elevated Mitochondrial Density Is Required for Normal Axon Regeneration

Are these axonal mitochondria important for regeneration? In mice, peripheral axon injury causes a global increase in the axonal transport of other factors in addition to mitochondria, including cytoskeleton components and metabolic enzymes (Mar et al., 2014; Misgeld et al., 2007). We used multiple approaches to focus specifically on axonal mitochondria. By measuring mitochondria and regeneration in single axons, we found that axons with low mitochondria density have poor

regeneration. By experimentally manipulating mitochondrial localization using two independent methods that are relatively specific to mitochondria (Miro and DRP1), we found that increasing mitochondria density is sufficient to increase regeneration, while reducing mitochondria density reduced regeneration. Furthermore, we found that experimentally inhibiting mitochondrial respiratory chain function also reduces regeneration. These results are consistent with a recent study demonstrating that the growth of cultured cortical neurons is enhanced by increasing mitochondrial motility and by ATP supplementation (Zhou et al., 2016). Together, these results indicate that, while multiple cellular components may be trafficked after nerve injury, axonal mitochondria have a specific and important function in axon regeneration.

Mitochondrial Function in Energy Production Is Critical for the Growth Phase of Axon Regeneration

Axon regeneration is a complex process, requiring injured neurons to generate injury signals, initiate a growth cone, and drive growth-cone migration over extended distances toward the postsynaptic target (El Bejjani and Hammarlund, 2012). We found that experimentally altering axonal mitochondria density does not affect growth-cone formation. Thus, injury signals and elaboration of growth cones after injury do not depend on axonal mitochondria. Rather, our data place the requirement for axonal mitochondria in the growth phase of the regeneration program, when injured axons are attempting to drive growth-cone migration.

Animals with an impaired mitochondrial respiratory chain have reduced oxygen consumption and reduced ATP levels, indicating reduced energy production. We found that these mutants have reduced axon regeneration. We also found that injured axons activate a reporter of energy stress, consistent with the idea that ATP generation by axonal mitochondria is critical to support regeneration. These data suggest that supplying energy is the major function of mitochondria during axon regeneration. Recent work in cultured cortical neurons supports this idea and further shows that axon injury can depolarize nearby mitochondria (Zhou et al., 2016). In regenerating axons, local ATP supply may depend on mitochondrial translocation within axons due to local mitochondrial depolarization (Zhou et al., 2016), the extended structure of axons, the limited diffusion ability of ATP (Hubley et al., 1995; Rostovtseva and Bezrukov, 1998; Sun et al., 2013), and ATP's short biological half-life (less than 1 s) (Mortensen et al., 2011). Axon regeneration requires a number of membrane trafficking steps (Bradke et al., 2012; Tuck and Cavalli, 2010), and these steps may be particularly sensitive to ATP levels (Rangaraju et al., 2014). Thus, although other aspects of axon regeneration may also require ATP, the growth phase depends strongly on ATP that must be supplied by axonal mitochondria.

DLK-1 Signaling Regulates Mitochondria Density after Injury

Axon injury generates injury signals that are received and transduced by signaling pathways, including the conserved DLK-1 regeneration pathway (Hammarlund et al., 2009; Shin et al., 2012; Xiong et al., 2010). However, the cellular effects of these signaling pathways, and how they mediate axon regeneration, are incompletely understood. Here we show that the DLK-1 pathway affects mitochondria density in injured axons. In the absence of injury, DLK-1 activation is sufficient to increase mitochondria density but does not change the distribution of other intracellular organelles. The ability of DLK-1 signaling to increase mitochondria density is largely dependent on the *cebp-1* transcription factor, suggesting that transcriptional regulation of target genes contributes to this process.

In injured neurons that lack DLK-1 signaling, the postinjury increase in mitochondria density is reduced, but not eliminated. Thus, DLK-1 signaling is part of the cellular pathway linking injury to mitochondria density, but other, unknown injury pathways function in parallel to perform this role. Beyond DLK-1 and AMPK, axon regeneration has been linked to diverse signaling factors, including NGF (Lindsay, 1988), Nogo (GrandPré et al., 2000), semaphorins (De Winter et al., 2002; Montolio et al., 2009), Roundabout-Slit (Chen et al., 2011), hippo (Nix et al., 2014), and PTEN (Byrne et al., 2014; Park et al., 2008; Sun et al., 2011). Many of these regulators also play roles in the regulation of mitochondria dynamics, function, or transport (Chada and Hollenbeck, 2004; Hollenbeck and Saxton, 2005; Nagaraj et al., 2012; Schwamborn et al., 2004; Sutendra et al., 2011; Thomas and Cookson, 2009). Further studies are necessary to determine the role of other pathways in the regulation of mitochondria density.

In summary, our results indicate that axon injury increases mitochondria density in injured axons, and these axonal mitochondria supply energy required for robust axon extension during axon regeneration. Our findings suggest that insufficient mitochondrial transport or energy production is one cause of failed axon regeneration and raise the possibility that promoting energy production might help to improve axon regeneration after injury.

EXPERIMENTAL PROCEDURES

Laser Axotomy and Axon Regeneration Analysis

Laser axotomy was performed as described previously (Byrne et al., 2011). Axons were scored for full regeneration to the dorsal nerve cord or regrowth over the dorsal-ventral midline. To determine the relative axon length, the distance from the ventral nerve cord to the injured axon end was normalized by the distance between ventral and dorsal nerve cords. Details can be found in the Supplemental Experimental Procedures.

Analysis of Mitochondria Density

Transgenic animals expressing Mito::GFP or mCherry were analyzed at the young adult stage (see Table S1). To assess mitochondria density in GABAergic neurons after axotomy, selected axons in transgenic animals expressing Mito::GFP or mCherry were cut using a Micropoint laser from Photonic Instruments (10 pulses, 20 Hz). The axotomized animals were recovered to NGM plates and cultured at 20°C. Then, 6, 12, or 24 hr later, images were acquired as 0.3~0.5 μm z stacks at room temperature on an UltraVIEW Vex (PerkinElmer) spinning-disc confocal microscope (Nikon Ti-E Eclipse inverted scope; Hamamatsu C9100-50 camera) with a 60× CFI Plan Apo numerical-aperture (NA) 1.4 oil-immersion objective using Volocity software (Improvision). To score mitochondria density, Mito::mCherry puncta in individual GABAergic axons were counted, and then the axon length was measured. The number of mitochondria was normalized by the axon length and converted to density per 100 μm axon length. To compare the volume of Mito::mCherry puncta, Volocity software (Improvision) was used to measure the volume of

individual puncta. All animals in each experiment were imaged on the same day with identical conditions, including camera gain, exposure settings, and fluorescence filters.

Selective Labeling of Mitochondria in the Ventral Nerve Cord by Photoconversion

The Dendra2 plasmid was generously provided by Dr. David Sherwood. Photoconversion was performed as previously described (Ihara et al., 2011). The ventral nerve cord of live transgenic animals was photoconverted and imaged using an UltraVIEW Vex (PerkinElmer) spinning-disc confocal microscope (Nikon Ti-E Eclipse inverted scope; Hamamatsu C9100-50 camera) with a 40× objective and Volocity FRAP Plugin (Improvision). Selected ventral nerve cord and cell bodies were scanned with a 405 nm laser at 1% power. The photoconverted red-Mito-Dendra2 within axons was captured immediately after photoconversion as 0.5 μm z stacks with a 60× objective. For experiments involving injured axons, GABA neurons were severed using a pulsed-laser axotomy and then photoconverted within about 5 min. Imaging immediately after axotomy did not show red-Mito::Dendra2 signal within the injured axon commissures. To test mitochondrial trafficking from the ventral nerve cord to the axons, animals with or without axotomy were recovered from the agar pad after photoconversion, cultured at 20°C for 24 hr, and then reimaged with identical settings using the 60× objective.

Analysis of PFK1.1 Clustering

After axotomy, animals were recovered on fresh NGM plates. Then, 24 hr after axotomy, animals were mounted, and images were acquired as 0.3 μm z stacks at room temperature within 10 min to minimize hypoxic effects. PFK-1.1::eGFP clustering was analyzed as described previously (Jang et al., 2016). Briefly, segmented-line scans were performed to measure fluorescence values for PFK-1.1::eGFP in individual axons using Volocity software (Improvision). Fluorescence peaks with higher values than 5,000 (a.u.) as a threshold were considered PFK-1.1::eGFP clusters.

SUPPLEMENTAL INFORMATION

Supplemental Information includes Supplemental Experimental Procedures, eight figures, and one table and can be found with this article online at http://dx.doi.org/10.1016/j.neuron.2016.11.025.

AUTHOR CONTRIBUTIONS

S.M.H. and M.H. designed the experiments, analyzed data, and wrote the manuscript. S.M.H. and H.S.B. conducted the experiments.

ACKNOWLEDGMENTS

We thank the *Caenorhabditis* Genetics Center Center (supported by the National Institutes of Health – Office of Research Infrastructure Programs; P40 OD010440) and the Mitani lab (Tokyo Women's Medical University School of Medicine) for strains, and also Dr. Cori Bargmann, Dr. Daniel Colon-Ramos, Dr. Siegfried Hekimi, and Dr. David R. Sherwood for plasmids or strains. We thank the Yale *C. elegans* community and the Yale axon regeneration group for advice on the project. We thank Sori Jang, Dr. Hieu Hoang, Dr. Sejin Lee, and members of the Hammarlund lab for advice and for sharing materials. S.M.H. was supported by the James Hudson Brown – Alexander Brown Coxe Postdoctoral Fellowships in the Medical Sciences and a Department of Genetics Research Fellowship from Yale University. Work in the Hammarlund lab is supported by NIH grants R01NS098817, R01NS094219, and R56AG050969.

Received: December 4, 2015
Revised: August 31, 2016
Accepted: November 8, 2016
Published: December 21, 2016

REFERENCES

Ahmad, T., Mukherjee, S., Pattnaik, B., Kumar, M., Singh, S., Kumar, M., Rehman, R., Tiwari, B.K., Jha, K.A., Barhanpurkar, A.P., et al. (2014). Miro1 regulates intercellular mitochondrial transport & enhances mesenchymal stem cell rescue efficacy. EMBO J. *33*, 994–1010.

Apfeld, J., O'Connor, G., McDonagh, T., DiStefano, P.S., and Curtis, R. (2004). The AMP-activated protein kinase AAK-2 links energy levels and insulin-like signals to lifespan in C. elegans. Genes Dev. *18*, 3004–3009.

Baughman, J.M., Perocchi, F., Girgis, H.S., Plovanich, M., Belcher-Timme, C.A., Sancak, Y., Bao, X.R., Strittmatter, L., Goldberger, O., Bogorad, R.L., et al. (2011). Integrative genomics identifies MCU as an essential component of the mitochondrial calcium uniporter. Nature *476*, 341–345.

Bradke, F., Fawcett, J.W., and Spira, M.E. (2012). Assembly of a new growth cone after axotomy: the precursor to axon regeneration. Nat. Rev. Neurosci. *13*, 183–193.

Byrne, A.B., Edwards, T.J., and Hammarlund, M. (2011). In vivo laser axotomy in C. elegans. JoVE *51*, 2707.

Byrne, A.B., Walradt, T., Gardner, K.E., Hubbert, A., Reinke, V., and Hammarlund, M. (2014). Insulin/IGF1 signaling inhibits age-dependent axon regeneration. Neuron *81*, 561–573.

Cai, Q., Zakaria, H.M., Simone, A., and Sheng, Z.H. (2012). Spatial parkin translocation and degradation of damaged mitochondria via mitophagy in live cortical neurons. Curr. Biol. *22*, 545–552.

Cartoni, R., Norsworthy, M.W., Bei, F., Wang, C., Li, S., Zhang, Y., Gabel, C.V., Schwarz, T.L., and He, Z. (2016). The mammalian specific protein Armcx1 regulates mitochondrial transport during axon regeneration. Neuron *92*, this issue, 1294–1307.

Case, L.C., and Tessier-Lavigne, M. (2005). Regeneration of the adult central nervous system. Curr. Biol. *15*, R749–R753.

Chada, S.R., and Hollenbeck, P.J. (2004). Nerve growth factor signaling regulates motility and docking of axonal mitochondria. Curr. Biol. *14*, 1272–1276.

Chang, D.T., and Reynolds, I.J. (2006). Mitochondrial trafficking and morphology in healthy and injured neurons. Prog. Neurobiol. *80*, 241–268.

Chen, L., Wang, Z., Ghosh-Roy, A., Hubert, T., Yan, D., O'Rourke, S., Bowerman, B., Wu, Z., Jin, Y., and Chisholm, A.D. (2011). Axon regeneration pathways identified by systematic genetic screening in C. elegans. Neuron *71*, 1043–1057.

Chisholm, A.D. (2013). Cytoskeletal dynamics in Caenorhabditis elegans axon regeneration. Annu. Rev. Cell Dev. Biol. *29*, 271–297.

Courchet, J., Lewis, T.L., Jr., Lee, S., Courchet, V., Liou, D.Y., Aizawa, S., and Polleux, F. (2013). Terminal axon branching is regulated by the LKB1-NUAK1 kinase pathway via presynaptic mitochondrial capture. Cell *153*, 1510–1525.

Curtis, R., O'Connor, G., and DiStefano, P.S. (2006). Aging networks in Caenorhabditis elegans: AMP-activated protein kinase (aak-2) links multiple aging and metabolism pathways. Aging Cell *5*, 119–126.

De Stefani, D., Raffaello, A., Teardo, E., Szabò, I., and Rizzuto, R. (2011). A forty-kilodalton protein of the inner membrane is the mitochondrial calcium uniporter. Nature *476*, 336–340.

De Winter, F., Oudega, M., Lankhorst, A.J., Hamers, F.P., Blits, B., Ruitenberg, M.J., Pasterkamp, R.J., Gispen, W.H., and Verhaagen, J. (2002). Injury-induced class 3 semaphorin expression in the rat spinal cord. Exp. Neurol. *175*, 61–75.

Detmer, S.A., and Chan, D.C. (2007). Functions and dysfunctions of mitochondrial dynamics. Nat. Rev. Mol. Cell Biol. *8*, 870–879.

El Bejjani, R., and Hammarlund, M. (2012). Neural regeneration in Caenorhabditis elegans. Annu. Rev. Genet. *46*, 499–513.

Firnhaber, C., and Hammarlund, M. (2013). Neuron-specific feeding RNAi in C. elegans and its use in a screen for essential genes required for GABA neuron function. PLoS Genet. *9*, e1003921.

Fransson, A., Ruusala, A., and Aspenström, P. (2003). Atypical Rho GTPases have roles in mitochondrial homeostasis and apoptosis. J. Biol. Chem. *278*, 6495–6502.

Goldberg, J.L. (2003). How does an axon grow? Genes Dev. *17*, 941–958.

GrandPré, T., Nakamura, F., Vartanian, T., and Strittmatter, S.M. (2000). Identification of the Nogo inhibitor of axon regeneration as a Reticulon protein. Nature *403*, 439–444.

Guo, X., Macleod, G.T., Wellington, A., Hu, F., Panchumarthi, S., Schoenfield, M., Marin, L., Charlton, M.P., Atwood, H.L., and Zinsmaier, K.E. (2005). The GTPase dMiro is required for axonal transport of mitochondria to Drosophila synapses. Neuron *47*, 379–393.

Hall, D.H., and Altun, Z.F. (2008). C. elegans atlas (Cold Spring Harbor Laboratory Press).

Hammarlund, M., Davis, W.S., and Jorgensen, E.M. (2000). Mutations in beta-spectrin disrupt axon outgrowth and sarcomere structure. J. Cell Biol. *149*, 931–942.

Hammarlund, M., Jorgensen, E.M., and Bastiani, M.J. (2007). Axons break in animals lacking beta-spectrin. J. Cell Biol. *176*, 269–275.

Hammarlund, M., Nix, P., Hauth, L., Jorgensen, E.M., and Bastiani, M. (2009). Axon regeneration requires a conserved MAP kinase pathway. Science *323*, 802–806.

Hardie, D.G. (2007). AMP-activated/SNF1 protein kinases: conserved guardians of cellular energy. Nat. Rev. Mol. Cell Biol. *8*, 774–785.

Hirokawa, N., Niwa, S., and Tanaka, Y. (2010). Molecular motors in neurons: transport mechanisms and roles in brain function, development, and disease. Neuron *68*, 610–638.

Hollenbeck, P.J., and Saxton, W.M. (2005). The axonal transport of mitochondria. J. Cell Sci. *118*, 5411–5419.

Hubert, T., Wu, Z., Chisholm, A.D., and Jin, Y. (2014). S6 kinase inhibits intrinsic axon regeneration capacity via AMP kinase in Caenorhabditis elegans. J. Neurosci. *34*, 758–763.

Hubley, M.J., Rosanske, R.C., and Moerland, T.S. (1995). Diffusion coefficients of ATP and creatine phosphate in isolated muscle: pulsed gradient 31P NMR of small biological samples. NMR Biomed. *8*, 72–78.

Hwang, A.B., and Lee, S.J. (2011). Regulation of life span by mitochondrial respiration: the HIF-1 and ROS connection. Aging (Albany, N.Y.) *3*, 304–310.

Ihara, S., Hagedorn, E.J., Morrissey, M.A., Chi, Q., Motegi, F., Kramer, J.M., and Sherwood, D.R. (2011). Basement membrane sliding and targeted adhesion remodels tissue boundaries during uterine-vulval attachment in Caenorhabditis elegans. Nat. Cell Biol. *13*, 641–651.

Jang, S., Nelson, J.C., Bend, E.G., Rodríguez-Laureano, L., Tueros, F.G., Cartagenova, L., Underwood, K., Jorgensen, E.M., and Colón-Ramos, D.A. (2016). Glycolytic Enzymes Localize to Synapses under Energy Stress to Support Synaptic Function. Neuron *90*, 278–291.

Kahn, B.B., Alquier, T., Carling, D., and Hardie, D.G. (2005). AMP-activated protein kinase: ancient energy gauge provides clues to modern understanding of metabolism. Cell Metab. *1*, 15–25.

Kerschensteiner, M., Schwab, M.E., Lichtman, J.W., and Misgeld, T. (2005). In vivo imaging of axonal degeneration and regeneration in the injured spinal cord. Nat. Med. *11*, 572–577.

Labrousse, A.M., Zappaterra, M.D., Rube, D.A., and van der Bliek, A.M. (1999). C. elegans dynamin-related protein DRP-1 controls severing of the mitochondrial outer membrane. Mol. Cell *4*, 815–826.

Lathrop, K.L., and Steketee, M.B. (2013). Mitochondrial dynamics in retinal ganglion cell axon regeneration and growth cone guidance. J. Ocul. Biol. *1*, 9.

Lee, H., Cho, J.S., Lambacher, N., Lee, J., Lee, S.J., Lee, T.H., Gartner, A., and Koo, H.S. (2008). The Caenorhabditis elegans AMP-activated protein kinase AAK-2 is phosphorylated by LKB1 and is required for resistance to oxidative stress and for normal motility and foraging behavior. J. Biol. Chem. *283*, 14988–14993.

Lee, S.J., Hwang, A.B., and Kenyon, C. (2010). Inhibition of respiration extends C. elegans life span via reactive oxygen species that increase HIF-1 activity. Curr. Biol. *20*, 2131–2136.

Lin, M.Y., and Sheng, Z.H. (2015). Regulation of mitochondrial transport in neurons. Exp. Cell Res. *334*, 35–44.

Lindsay, R.M. (1988). Nerve growth factors (NGF, BDNF) enhance axonal regeneration but are not required for survival of adult sensory neurons. J. Neurosci. *8*, 2394–2405.

Mar, F.M., Simões, A.R., Leite, S., Morgado, M.M., Santos, T.E., Rodrigo, I.S., Teixeira, C.A., Misgeld, T., and Sousa, M.M. (2014). CNS axons globally increase axonal transport after peripheral conditioning. J. Neurosci. *34*, 5965–5970.

Martin, L.J., Kaiser, A., and Price, A.C. (1999). Motor neuron degeneration after sciatic nerve avulsion in adult rat evolves with oxidative stress and is apoptosis. J. Neurobiol. *40*, 185–201.

Miller, K.E., and Sheetz, M.P. (2004). Axonal mitochondrial transport and potential are correlated. J. Cell Sci. *117*, 2791–2804.

Misgeld, T., Kerschensteiner, M., Bareyre, F.M., Burgess, R.W., and Lichtman, J.W. (2007). Imaging axonal transport of mitochondria in vivo. Nat. Methods *4*, 559–561.

Montolio, M., Messeguer, J., Masip, I., Guijarro, P., Gavin, R., Antonio Del Río, J., Messeguer, A., and Soriano, E. (2009). A semaphorin 3A inhibitor blocks axonal chemorepulsion and enhances axon regeneration. Chem. Biol. *16*, 691–701.

Morris, R.L., and Hollenbeck, P.J. (1993). The regulation of bidirectional mitochondrial transport is coordinated with axonal outgrowth. J. Cell Sci. *104*, 917–927.

Mortensen, S.P., Thaning, P., Nyberg, M., Saltin, B., and Hellsten, Y. (2011). Local release of ATP into the arterial inflow and venous drainage of human skeletal muscle: insight from ATP determination with the intravascular microdialysis technique. J. Physiol. *589*, 1847–1857.

Nagaraj, R., Gururaja-Rao, S., Jones, K.T., Slattery, M., Negre, N., Braas, D., Christofk, H., White, K.P., Mann, R., and Banerjee, U. (2012). Control of mitochondrial structure and function by the Yorkie/YAP oncogenic pathway. Genes Dev. *26*, 2027–2037.

Nakata, K., Abrams, B., Grill, B., Goncharov, A., Huang, X., Chisholm, A.D., and Jin, Y. (2005). Regulation of a DLK-1 and p38 MAP kinase pathway by the ubiquitin ligase RPM-1 is required for presynaptic development. Cell *120*, 407–420.

Nix, P., Hammarlund, M., Hauth, L., Lachnit, M., Jorgensen, E.M., and Bastiani, M. (2014). Axon regeneration genes identified by RNAi screening in C. elegans. J. Neurosci. *34*, 629–645.

Palikaras, K., Lionaki, E., and Tavernarakis, N. (2015). Coordination of mitophagy and mitochondrial biogenesis during ageing in C. elegans. Nature *521*, 525–528.

Park, K.K., Liu, K., Hu, Y., Smith, P.D., Wang, C., Cai, B., Xu, B., Connolly, L., Kramvis, I., Sahin, M., and He, Z. (2008). Promoting axon regeneration in the adult CNS by modulation of the PTEN/mTOR pathway. Science *322*, 963–966.

Rangaraju, V., Calloway, N., and Ryan, T.A. (2014). Activity-driven local ATP synthesis is required for synaptic function. Cell *156*, 825–835.

Rawson, R.L., Yam, L., Weimer, R.M., Bend, E.G., Hartwieg, E., Horvitz, H.R., Clark, S.G., and Jorgensen, E.M. (2014). Axons degenerate in the absence of mitochondria in C. elegans. Curr. Biol. *24*, 760–765.

Rieger, S., and Sagasti, A. (2011). Hydrogen peroxide promotes injury-induced peripheral sensory axon regeneration in the zebrafish skin. PLoS Biol. *9*, e1000621.

Rostovtseva, T.K., and Bezrukov, S.M. (1998). ATP transport through a single mitochondrial channel, VDAC, studied by current fluctuation analysis. Biophys. J. *74*, 2365–2373.

Runkel, E.D., Liu, S., Baumeister, R., and Schulze, E. (2013). Surveillance-activated defenses block the ROS-induced mitochondrial unfolded protein response. PLoS Genet. *9*, e1003346.

Saotome, M., Safiulina, D., Szabadkai, G., Das, S., Fransson, A., Aspenstrom, P., Rizzuto, R., and Hajnóczky, G. (2008). Bidirectional Ca2+-dependent control of mitochondrial dynamics by the Miro GTPase. Proc. Natl. Acad. Sci. USA *105*, 20728–20733.

Schwamborn, J.C., Fiore, R., Bagnard, D., Kappler, J., Kaltschmidt, C., and Püschel, A.W. (2004). Semaphorin 3A stimulates neurite extension and regulates gene expression in PC12 cells. J. Biol. Chem. *279*, 30923–30926.

Sheng, Z.H. (2014). Mitochondrial trafficking and anchoring in neurons: New insight and implications. J. Cell Biol. *204*, 1087–1098.

Shin, J.E., Cho, Y., Beirowski, B., Milbrandt, J., Cavalli, V., and DiAntonio, A. (2012). Dual leucine zipper kinase is required for retrograde injury signaling and axonal regeneration. Neuron *74*, 1015–1022.

Spillane, M., Ketschek, A., Merianda, T.T., Twiss, J.L., and Gallo, G. (2013). Mitochondria coordinate sites of axon branching through localized intra-axonal protein synthesis. Cell Rep. *5*, 1564–1575.

Steketee, M.B., Moysidis, S.N., Weinstein, J.E., Kreymerman, A., Silva, J.P., Iqbal, S., and Goldberg, J.L. (2012). Mitochondrial dynamics regulate growth cone motility, guidance, and neurite growth rate in perinatal retinal ganglion cells in vitro. Invest. Ophthalmol. Vis. Sci. *53*, 7402–7411.

Sun, F., Park, K.K., Belin, S., Wang, D., Lu, T., Chen, G., Zhang, K., Yeung, C., Feng, G., Yankner, B.A., and He, Z. (2011). Sustained axon regeneration induced by co-deletion of PTEN and SOCS3. Nature *480*, 372–375.

Sun, T., Qiao, H., Pan, P.Y., Chen, Y., and Sheng, Z.H. (2013). Motile axonal mitochondria contribute to the variability of presynaptic strength. Cell Rep. *4*, 413–419.

Sutendra, G., Dromparis, P., Wright, P., Bonnet, S., Haromy, A., Hao, Z., McMurtry, M.S., Michalak, M., Vance, J.E., Sessa, W.C., and Michelakis, E.D. (2011). The role of Nogo and the mitochondria-endoplasmic reticulum unit in pulmonary hypertension. Sci. Transl. Med. *3*, 88ra55.

Tawe, W.N., Eschbach, M.L., Walter, R.D., and Henkle-Dührsen, K. (1998). Identification of stress-responsive genes in Caenorhabditis elegans using RT-PCR differential display. Nucleic Acids Res. *26*, 1621–1627.

Thomas, K.J., and Cookson, M.R. (2009). The role of PTEN-induced kinase 1 in mitochondrial dysfunction and dynamics. Int. J. Biochem. Cell Biol. *41*, 2025–2035.

Tuck, E., and Cavalli, V. (2010). Roles of membrane trafficking in nerve repair and regeneration. Commun. Integr. Biol. *3*, 209–214.

Verburg, J., and Hollenbeck, P.J. (2008). Mitochondrial membrane potential in axons increases with local nerve growth factor or semaphorin signaling. J. Neurosci. *28*, 8306–8315.

Verstreken, P., Ly, C.V., Venken, K.J., Koh, T.W., Zhou, Y., and Bellen, H.J. (2005). Synaptic mitochondria are critical for mobilization of reserve pool vesicles at Drosophila neuromuscular junctions. Neuron *47*, 365–378.

Wakabayashi, J., Zhang, Z., Wakabayashi, N., Tamura, Y., Fukaya, M., Kensler, T.W., Iijima, M., and Sesaki, H. (2009). The dynamin-related GTPase Drp1 is required for embryonic and brain development in mice. J. Cell Biol. *186*, 805–816.

Wang, X., Winter, D., Ashrafi, G., Schlehe, J., Wong, Y.L., Selkoe, D., Rice, S., Steen, J., LaVoie, M.J., and Schwarz, T.L. (2011). PINK1 and Parkin target Miro for phosphorylation and degradation to arrest mitochondrial motility. Cell *147*, 893–906.

Xiong, X., Wang, X., Ewanek, R., Bhat, P., Diantonio, A., and Collins, C.A. (2010). Protein turnover of the Wallenda/DLK kinase regulates a retrograde response to axonal injury. J. Cell Biol. *191*, 211–223.

Xu, S., and Chisholm, A.D. (2014). C. elegans epidermal wounding induces a mitochondrial ROS burst that promotes wound repair. Dev. Cell *31*, 48–60.

Yan, D., and Jin, Y. (2012). Regulation of DLK-1 kinase activity by calcium-mediated dissociation from an inhibitory isoform. Neuron *76*, 534–548.

Yan, D., Wu, Z., Chisholm, A.D., and Jin, Y. (2009). The DLK-1 kinase promotes mRNA stability and local translation in C. elegans synapses and axon regeneration. Cell *138*, 1005–1018.

Yang, W., and Hekimi, S. (2010). A mitochondrial superoxide signal triggers increased longevity in Caenorhabditis elegans. PLoS Biol. *8*, e1000556.

Yang, W., Li, J., and Hekimi, S. (2007). A measurable increase in oxidative damage due to reduction in superoxide detoxification fails to shorten the life span of long-lived mitochondrial mutants of Caenorhabditis elegans. Genetics *177*, 2063–2074.

Yanik, M.F., Cinar, H., Cinar, H.N., Chisholm, A.D., Jin, Y., and Ben-Yakar, A. (2004). Neurosurgery: functional regeneration after laser axotomy. Nature *432*, 822.

Yee, C., Yang, W., and Hekimi, S. (2014). The intrinsic apoptosis pathway mediates the pro-longevity response to mitochondrial ROS in C. elegans. Cell *157*, 897–909.

Zhou, B., Yu, P., Lin, M.Y., Sun, T., Chen, Y., and Sheng, Z.H. (2016). Facilitation of axon regeneration by enhancing mitochondrial transport and rescuing energy deficits. J. Cell Biol. *214*, 103–119.